



Indian Journal of Chemistry
Vol. 59A, June 2020, pp. 760-767



Thermodynamic and kinetic studies on novel Platinum(II) Complex containing bidentate N,N-donor ligands in ethanol-water medium

Debabrata Nandi^a, Parnajyoti Karmakar^b, Anwasha Dey^a, Roshni Sarkar (Sain)^a & Alak K. Ghosh^{a*}

^aDepartment of Chemistry, The University of Burdwan, Purba Bardhaman-713 104, West Bengal, India.

^bGovernment General Degree College at Kalna-1, Muragacha, Medgachi, Burdwan-713 405, West Bengal, India

*Email: alakghosh2002@yahoo.co.in

Received 09 August 2019; revised and accepted 22 April 2020

Kinetic and mechanistic investigations have been made on the displacement of the two aqua molecules from the complex **1** i.e., $[\text{Pt}(2,2'\text{-bipyridine})(\text{H}_2\text{O})_2]^{2+}$ represented as $\{\text{Pt}(\text{bpy})\}$ (bpy = 2,2'-bipyridine) at pH 4.0. All the substitution reactions have been monitored at 264, 284 & 317 nm, where the spectral difference between the reactant and product is maximum. Two consecutive reaction steps have been observed for the substitution of aqua molecules with some bidentate N,N-donor ligands namely, dimethylglyoxime (L_1H), 1, 2-cyclohexanedionedioxime (L_2H) and α -furildioxime (L_3H) in ethanol-water medium using variable-temperature and stopped-flow spectrophotometry. Among the two steps, the former is ligand dependent and the later is ligand independent, where chelation is observed. All rate and activation parameters are consistent with associative substitution mechanisms. The thermodynamic parameters have been also calculated, which gives a negative ΔG^0 value at all temperatures studied, supporting the spontaneous formation of an outer sphere association complex. The products of the reaction have been characterized with the help of IR and ESI-MS spectroscopic analysis.

Keywords : Kinetics, Platinum(II) complexes, 2,2'-Bipyridine, Vicinal dioximes

Cis-diamminedichloroplatinum(II) (cisplatin) has been established as the leading compound for the treatment of different types of cancer. It is highly effective in the treatment of testicular and ovarian cancers and is also employed for treating bladder, cervical, head and neck, oesophageal, and small cell lung cancer¹. However, some tumors such as colorectal and non small cell lung cancers have intrinsic resistance to cisplatin, while others such as ovarian or small cell lung cancers develop acquired resistance after the initial treatment². Biochemical studies have not clearly established the molecular bases of resistance to cisplatin in any type of cell, but, at least, they have identified several mechanisms that can contribute to this phenomenon. Resistance to cisplatin is generally multifactorial and has been shown to be due to reduced drug accumulation, inactivation by thiol containing species, increased repair/tolerance of platinum-DNA adducts, and alterations in proteins involved in apoptosis^{3,4}.

One strategy to overcome cisplatin resistance is to design platinum complexes that specifically deal with some or even all of the above-mentioned resistance mechanisms. Further studies in this field revealed a number of different Pt(II) complexes, structurally

similar to cisplatin, with reduced toxicity, but still not suitable for longer application⁵⁻⁷. To date, about 3000 different platinum complexes have been synthesized and investigated in an attempt to improve the antitumor activity, to lower the toxicity and to design a drug that is able to overcome cell resistance. However, only about 30 platinum complexes have hitherto entered clinical trials⁸⁻¹⁰. Moreover, only four platinum drugs namely; cisplatin, carboplatin, oxaliplatin and nedaplatin are currently registered for clinical use (marketed drugs)¹¹. Among the registered platinum drugs, carboplatin, [*cis*-diammine-1,1'-cyclobutanedicarboxylateplatinum(II)], is less toxic than cisplatin but possesses the same spectrum of antitumor activity. The only registered platinum drug that has consistently demonstrated antitumor activity against cisplatin resistant tumors such as colorectal cancers is oxaliplatin, [*trans*-L-1,2-diaminocyclohexaneoxalatoplatinum(II)]¹².

However, there have been recently reported several novel classes of platinum complexes able to circumvent cisplatin resistance in preclinical or even clinical studies including *cis*-Pt(II) compounds with planar ligands, *trans*-Pt(II) and *trans*-Pt(IV) compounds, and polynuclear platinum complexes¹³.

Taking into account the above-mentioned considerations, there is little doubt that the search for novel platinum compounds able to circumvent cisplatin resistance has proven to be a difficult task. The coordination compounds of vicinal dioximes have been widely investigated as analytical reagents¹⁴, models for biological systems such as vitamin B12¹⁵, compounds with columnar stacking thought to be behind their semiconducting properties¹⁶ and recently effective new dioxygen carriers¹⁷. In this study, the reactions of Pt(bpy) with some bidentate N, N-donor ligands viz., dimethylglyoxime (L₁H), 1,2-cyclohexanedionedioxime (L₂H) and α -furildioxime (L₃H) were investigated by stopped-flow spectrophotometry.

Materials and Methods

K₂PtCl₄, 2,2'-bipyridine and vicinal dioximes were purchased from Sigma-Aldrich Company. All other reagents were obtained from commercial sources and used without purification. All kinetics studies were performed in 10% ethanol-water (v/v) mixture. The complex [Pt(bpy)(H₂O)₂](ClO₄)₂ termed as complex **1**, was prepared in our previous paper according to the literature^{18,23}. The pH of the solution was so maintained (pH = 4.0) that more than 90% of the perchlorate salt was obtained as diaqua species. The reaction products of complex **1** with the above three vicinal dioximes (LH) were prepared by mixing the reactants in different ratio's namely 1:5, 1:10, 1:20 and 1:30 and equilibrating the mixture at (30 ± 0.1) °C for 48 h. The absorption spectra of all these mixtures for each individual ligand exhibited the same λ_{\max} with nearly identical intensities. The difference in spectra between the product complexes and the substrate complex is shown in Fig. 1.

The pH measurements were carried out with the help of a Sartorius Digital pH meter (model PB11) with an accuracy of ±0.01 units. Infrared (IR) spectroscopy on KBr pellets was performed on a Shimadzu FT-IR model IR Prestige 21 infrared spectrophotometer from 4,000 to 400 cm⁻¹. ESI-MS were recorded using a micromass Q-ToF microTM mass spectrometer in positive ion mode. Electronic spectra (UV/visible) and kinetic measurements were monitored in a Hi-Tech stopped flow spectrophotometer (TGK Scientific, Bradford-on-Avon, UK).

Job's measurements

The composition in the solution was determined by Job's method of continuous variation. The

metal:ligand ratio was found to be 1:1 (Fig. 2). When another two ligands react with the complex **1**, this ratio is also observed. As indicated from Job's method, complex **1** and the ligands were mixed in 1:1 molar ratio at pH 4.0 heated at 60 °C for 72 h, then transferred in a glass beaker and slowly evaporated at room temperature and finally in a desiccators. The yellowish products obtained were used for IR and ESI-MS spectroscopic analysis.

IR spectral analysis

The IR spectrum of the product, complex **1** with that of L₂H (in KBr disk) showed (Supplementary Data, Fig. S1) strong characteristic bands at

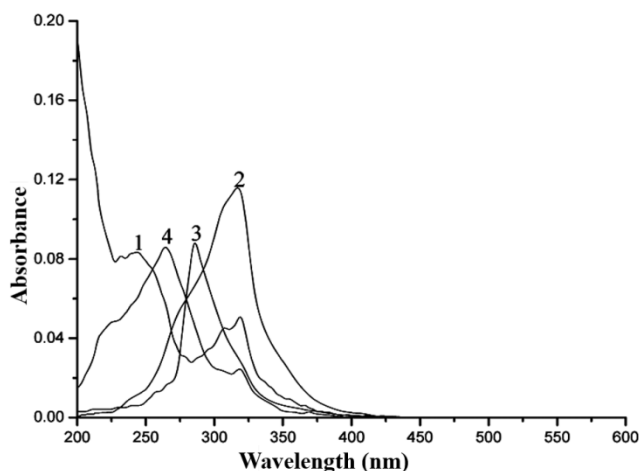


Fig. 1 — Spectra of the starting complex. [complex **1**] = 3.7×10^{-5} mol dm⁻³ (1), complex **1** + [α -furil dioxime] = 7.4×10^{-4} mol dm⁻³ (2), complex **1** + [1, 2-cyclohexanedionedioxime] = 7.4×10^{-4} mol dm⁻³ (3) and the last one is complex **1** with that of [dimethylglyoxime] = 7.4×10^{-4} mol dm⁻³ (4) at pH = 4.0, 10% ethanol-water (v/v) solution.

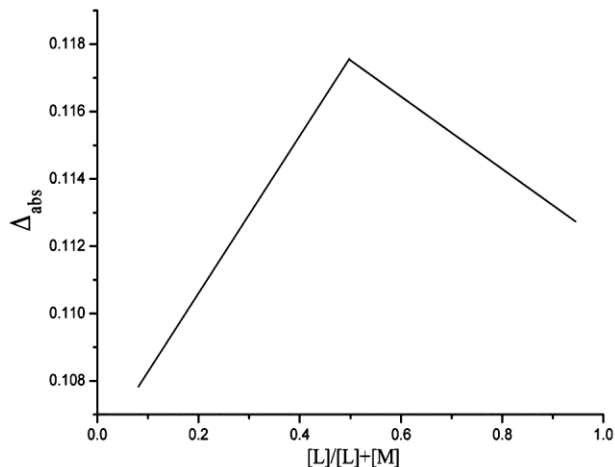


Fig. 2 — Job's plot for the reaction of complex **1** with L₂H at pH = 4.0 and ionic strength = 0.1 mol dm⁻³ NaClO₄.

3323 and 528 cm^{-1} , respectively. The strong band at 3323 cm^{-1} indicates that the product is hydrated or contained free -OH group. The stretching frequency at 528 cm^{-1} is assigned to $\nu(\text{Pt-N})$ bond in the product¹⁹. The absence of a strong band due to Pt-O bond at 617 cm^{-1} ²⁰, present in starting complex **1** (Supplementary Data, Fig. S2) suggests the absence of Pt-O bond in the product complex. So the IR spectrum strongly suggests that the final product is an N, N coordinated chelate and the 1,2-cyclohexanedionedioxime behaves as a bidentate ligand in the experimental pH.

Mass spectral analysis

The ESI mass spectra of the products have shown in Supplementary Data, Figs. S3 & S4. It is clear from the first spectrum that the ion at $m/z \sim 466$ has become the molecular ion species in the solution mixture and this is attributed to [Pt(II)+bpy+dimethylglyoxime anion]. On the other hand, in the second spectrum the ion at $m/z \sim 615$ has become the molecular ion species in the solution mixture and this is attributed to [Pt(II)+bpy+1,2-cyclohexanedionedioxime anion + NaClO_4].

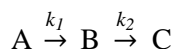
Kinetic measurements

The kinetic measurements of these systems were monitored in a Hi-Tech stopped flow spectrophotometer (TGM Scientific, Bradford-on-Avon, UK). The conventional mixing technique was followed and pseudo-first order conditions were employed throughout. The progress of the reaction was studied by following the development of peaks at 264, 284 and 317 nm for L_1H , L_2H and L_3H , respectively, where the differences in absorbance between the substrate and the product complexes are

maximum. Origin software was used for computational analysis. Rate data, represented as an average of duplicate runs, were reproducible to within $\pm 4\%$. The kinetic measurements of these systems were done as discussed in our previous work¹⁸. In this paper the nature of the two typical plots $\{\ln(A_\infty - A_t)\}$ vs time and $\ln \Delta$ vs time are also the same as discussed in our previous work¹⁸.

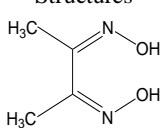
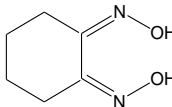
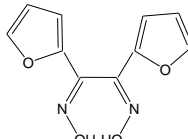
Results and Discussion

The pK_a values at 25 °C of the ligands L_1H , L_2H and L_3H are given in Table 1. From the pK_a values of all the ligands we can say that at pH 4.0, all these three ligands remain in the neutral form. On the other hand the pK_1 & pK_2 values for $\text{cis-}[\text{Pt}(\text{bpy})(\text{H}_2\text{O})_2]^{2+}$ have been evaluated by Irving-Rossotti technique²² and found to be 4.80, 6.32, respectively at 25 °C. Hence it can be assumed that at pH 4.0, the reactant complex exists as diaqua ion. The reactions followed two-step consecutive process; the first step is dependent on ligand concentration whereas the second is independent of ligand concentration. In the first step one aqua ligand was replaced from complex **1** by ligands. The second is a slower step, where another water molecule is substituted. This is the ring closure step. The rate constant for such a process can be evaluated by assuming the following scheme:



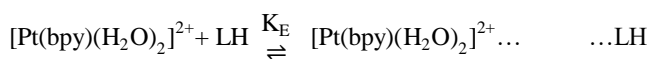
where A is the diaqua species (complex **1**), B is the single substituted intermediate, C is the final chelated product complex $[\text{Pt}(\text{bpy})(L)]^+$. Formation of C from B is predominant after some time has elapsed.

Table 1 — pK_a values of three ligands named Dimethylglyoxime (L_1H), 1, 2-Cyclohexane dionedioxime (L_2H) & α -Furildioxime (L_3H) at 25°C

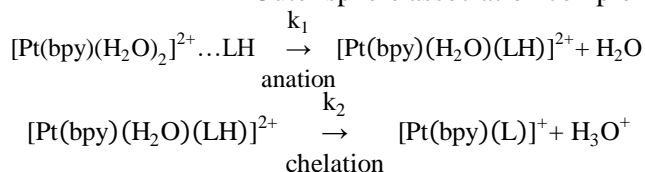
Ligands	Structures	Reference
Dimethylglyoxime (L_1H) $pK_1 = 10.66$		21
1,2-Cyclohexane dionedioxime (L_2H) $pK_1 = 12$		21
α -Furildioxime (L_3H) $pK_1 = 11.5$		21

Calculation of k_1 for A \rightarrow B step

The rate constants for the first step of the reaction (A \rightarrow B) were calculated from the absorbance data using the origin 6.0 software. The $k_{I(\text{obs})}$ values for different concentrations of ligand at different temperatures are given in Table 2. The rate increases for the above complex with increases in [ligand] before reaching a limiting value (Figs. 3, S5 & S6), which is probably due to the completion of the outer-sphere association complex formation through H-bonding. Based on the experimental findings, the following scheme may be proposed:



Outer sphere association complex



where, LH is the neutral form of the above ligands. Based on the above scheme, a rate expression can be derived for the A \rightarrow B step;

$$\frac{d[\text{B}]}{dt} = k_I K_E [\text{A}][\text{LH}] \quad \dots(1)$$

where A is the diaqua species (complex 1), B is the single substituted intermediate and LH is neutral ligand.

$$K_E = \frac{[\text{associated A}]}{[\text{A}][\text{LH}]}$$

$$\text{or, } [\text{associated A}] = K_E [\text{A}][\text{LH}]$$

$$[\text{A}]_T = [\text{A}] + [\text{associated A}]$$

$$\text{or, } [\text{A}]_T = [\text{A}] + K_E [\text{A}][\text{LH}]$$

$$\text{or, } [\text{A}] = \frac{[\text{A}]_T}{1 + K_E [\text{LH}]} \quad \dots(2)$$

Putting the value of [A] in Eqn 1, we get

$$\frac{d[\text{B}]}{dt} = \frac{k_I K_E [\text{LH}][\text{A}]_T}{1 + K_E [\text{LH}]}$$

$$\text{and } \frac{d[\text{B}]}{dt} = k_{I(\text{obs})} [\text{A}]_T; \text{ where T is total concentration of A}$$

$$\text{Thus it can be written as, } k_{I(\text{obs})} = \frac{k_I K_E [\text{LH}]}{1 + K_E [\text{LH}]}$$

The equation can be represented as

$$1/k_{I(\text{obs})} = 1/k_I + 1/k_I K_E [\text{LH}] \quad \dots(3)$$

Depending upon the above final equation, we have drawn a figure of $1/k_{I(\text{obs})}$ versus $1/[\text{LH}]$. The plot is

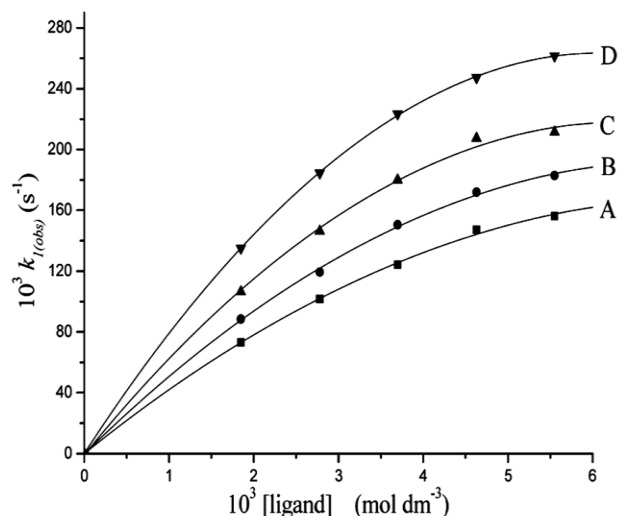


Fig. 3 — Plots of $k_{I(\text{obs})}$ (s^{-1}) versus $[\text{L}_1\text{H}]$ (mol dm^{-3}) at different temperatures. A = 40 °C, B = 45 °C, C = 50 °C and D = 55 °C.

Table 2 — $10^2 k_{I(\text{obs})}$ (s^{-1}) values for different concentrations of ligands at different temperatures; $[\text{cis-}[\text{Pt}(\text{bpy})(\text{H}_2\text{O})_2]^{2+}] = 1.85 \times 10^{-4} \text{ mol dm}^{-3}$, pH = 4.0, ionic strength = 0.1 mol dm^{-3} NaClO_4 , in 10% ethanol-water (v/v) mixture

Ligand	Temp. (°C)	10^3 [ligand] (mol dm^{-3})				
		1.85	2.78	3.70	4.63	5.55
L_1H	40	7.32±0.01	10.15±0.03	12.42±0.02	14.70±0.04	15.62±0.03
	45	8.84±0.04	11.94±0.02	15.05±0.03	17.19±0.05	18.28±0.01
	50	10.64±0.03	14.63±0.02	17.99±0.01	20.74±0.04	21.13±0.03
	55	13.52±0.01	18.46±0.04	22.36±0.03	24.73±0.02	26.17±0.01
L_2H	40	6.03±0.04	8.22±0.01	10.07±0.02	11.43±0.03	12.33±0.05
	45	7.54±0.02	10.29±0.03	12.30±0.04	13.81±0.01	15.20±0.05
	50	9.51±0.05	12.8±0.01	15.3±0.03	17.24±0.04	18.64±0.01
	55	11.89±0.03	15.89±0.04	18.9±0.01	20.58±0.05	22.80±0.03
L_3H	40	4.77±0.04	6.48±0.01	7.82±0.03	9.07±0.04	10.31±0.01
	45	6.33±0.03	8.49±0.02	10.27±0.04	11.66±0.01	13.45±0.03
	50	7.66±0.05	10.18±0.04	12.43±0.03	13.95±0.02	15.79±0.01
	55	10.26±0.04	13.63±0.03	16.57±0.01	18.17±0.04	20.32±0.03

linear with an intercept of $1/k_1$ and slope $1/k_1K_E$. This was found to be so, at all temperatures studied (Figs. 4, S7 & S8). The values of k_1 and K_E were obtained from the intercept and slope to intercept ratio respectively, and are included in Table 3.

Calculation of k_2 for B \rightarrow C step

The B \rightarrow C step is assigned to ring closure where another nitrogen atom of those ligands binds the metal center. This chelation step is independent of ligand concentration. At each temperature, the k_2 values were calculated from the limiting linear portion (when t is large) of the $\ln(A_\infty - A_t)$ versus t curves and are collected in Table 3.

Effect of pH on the reaction rate

The reaction was studied at five different pH values. At a fixed 1.85×10^{-4} mol dm $^{-3}$ [complex 1], 3.7×10^{-3} mol dm $^{-3}$ [ligand] and 0.1 mol dm $^{-3}$ NaClO $_4$ ionic strength, the $10^2k_{1(\text{obs})}$ values were 7.25,

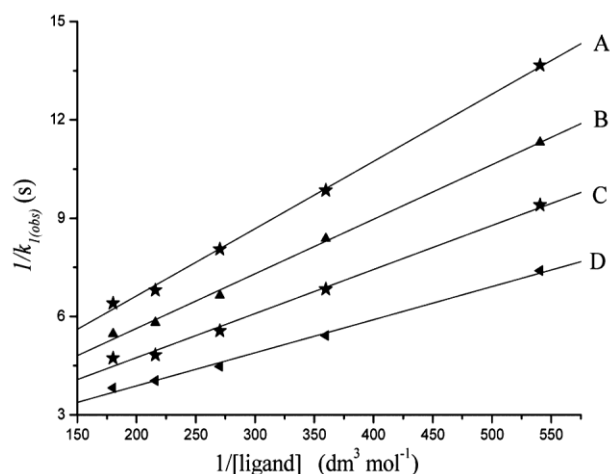


Fig. 4 — Plots of $1/k_{1(\text{obs})}$ (s) versus $1/[L_1H]$ (dm 3 mol $^{-1}$) at different temperatures A = 40 °C, B = 45 °C, C = 50 °C and D = 55 °C for complex 1.

8.91, 10.07, 11.51, 12.99 and 10^4k_2 values were 1.19, 1.45, 1.81, 2.19, 2.61, respectively for complex 1 with that of L $_2$ H at pH 3.0, 3.5, 4.0, 4.5 and 5.0, respectively at 40 °C. The change in rate may be explained based on two acid dissociation equilibria of the ligand and for the complex. Within our studied pH range the above ligands, remain unchanged so the effects of pH on rate are therefore due to the change in reactive forms of the reacting complex.

Effect of substituents in the ligand frame

If two methyl groups in L $_1$ H are successively replaced by cyclohexane ring in L $_2$ H and two furan rings in L $_3$ H, the substituent effect shows that there is a gradual decrease of rate constant values from L $_1$ H to L $_3$ H through L $_2$ H. For L $_1$ H, L $_2$ H and L $_3$ H, the relative λ_{max} positions of LH substituted products are found to be 264, 284 & 317 nm, respectively (Fig. 1). It decides a clear evidence of weak donicity trend as a sharp lower energy shift of λ_{max} position in going from complexed L $_1$ H to L $_3$ H through L $_2$ H. The measurement of rate constant values depends on both electronic and steric factors. For an associative activation with increase in the size of the incoming ligand, the activated state is crowded and as a result a decrease in rate with increased crowding is observed. This also supports a ligand assisted mechanism.

Effects of temperature on reaction rate

Those reactions were monitored at four different temperatures for diverse ligand concentrations and the substitution rate constants for both A \rightarrow B (k_1) and B \rightarrow C (k_2) steps are arranged in Table 3. The activation parameters calculated from Eyring plots (Figs. 5, S9 & S10) are tabulated in Table 4.

Mechanism

The interaction of dimethylglyoxime (L $_1$ H), 1,2-cyclohexane dionedioxime (L $_2$ H) and α -fural

Table 3 — The k_1 , K_E and k_2 values for the substitution reaction between different ligands with complex 1

Ligands	Temp. (°C)	10^2k_1 (s $^{-1}$)	K_E (dm 3 mol $^{-1}$)	10^4k_2 (s $^{-1}$)
L $_1$ H	40	39.59±0.03	123±0.02	2.51±0.01
	45	43.29±0.04	139±0.01	3.13±0.03
	50	48.58±0.01	153±0.03	4.06±0.02
	55	53.59±0.05	185±0.02	5.22±0.01
L $_2$ H	40	27.41±0.04	153±0.02	1.81±0.04
	45	31.34±0.01	172±0.03	2.39±0.03
	50	37.03±0.02	188±0.05	3.21±0.02
	55	42.14±0.03	214±0.04	4.44±0.01
L $_3$ H	40	23.40±0.02	138±0.01	1.17±0.04
	45	28.43±0.01	154±0.04	1.95±0.05
	50	32.47±0.05	166±0.02	2.98±0.01
	55	39.57±0.04	189±0.03	4.24±0.02

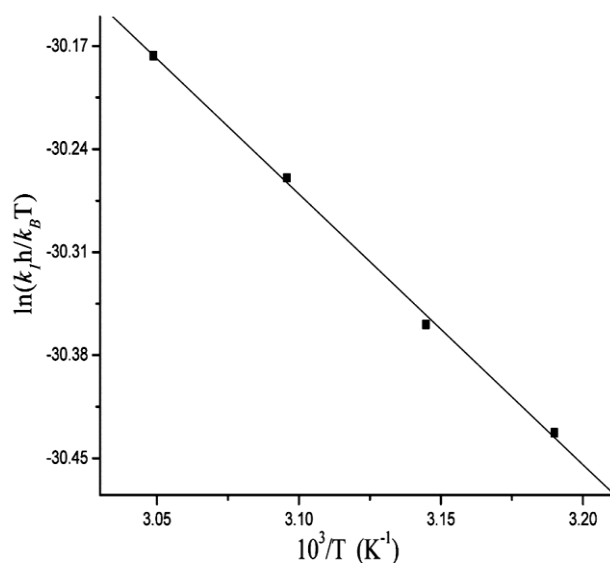


Fig. 5 — Eyring plot of $\ln(k_1h/k_B T)$ versus $1/T$ for the step $A \rightarrow B$ (For complex 1 with L_1H).

dioxime (L_3H) with the title platinum complex proceeds via two distinct consecutive steps ($k_1 \sim 10^{-2} \text{ s}^{-1}$ and $k_2 \sim 10^{-4} \text{ s}^{-1}$). First step proceeds via an associative interchange activation and the second step is the ring closure. At the outset of first step outer sphere association complex results, this is stabilized through H-bonding and is followed by an interchange from the outer sphere to the inner sphere complex. The outer sphere association equilibrium constants, a measure of the extent of H-bonding at different temperatures are evaluated (Table 3). A typical plot of $\ln K_E$ vs $1/T$ for complex 1 with L_2H is drawn in supplementary data, Fig. S11. From the slope and intercept values the thermodynamic parameters (ΔH^0 & ΔS^0) were also calculated (Supplementary Data, Table S1), which gives a negative ΔG^0 value at all temperatures studied, supporting the spontaneous formation of an outer sphere association complex in the first step.

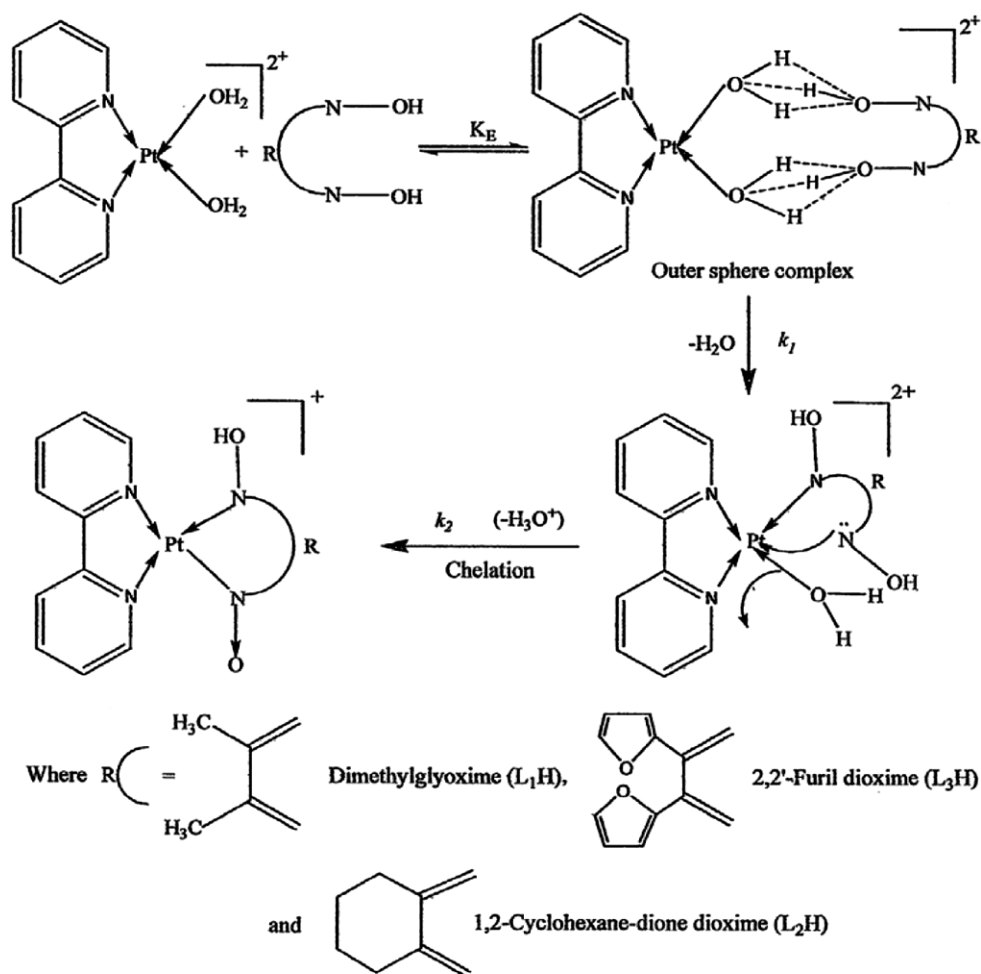


Fig. 6 — Plausible mechanism for the substitution of aqua ligands from $[Pt(bpy)(H_2O)_2]^{2+}$ by three vicinal dioxime.

Table 4 — Activation parameters for the analogous system by the above three vicinal dioximes

Systems	ΔH_1^\ddagger (kJ mol ⁻¹)	ΔS_1^\ddagger (J K ⁻¹ mol ⁻¹)	ΔH_2^\ddagger (kJ mol ⁻¹)	ΔS_2^\ddagger (J K ⁻¹ mol ⁻¹)	Ref.	
[Pt(en)(H ₂ O) ₂]	/L ₁ H	20.9 ± 1.5	-164 ± 4	31.6 ± 2.3	-226 ± 7	23
	/L ₂ H	27.4 ± 1.9	-214 ± 9	35.2 ± 3.4	-218 ± 11	
	/L ₃ H	30.6 ± 1.7	-205 ± 5	38.4 ± 2.3	-209 ± 7	
[Pt(pipen)(H ₂ O) ₂] ²⁺	/L ₁ H	35.6 ± 4.8	-182 ± 15	41.3 ± 2.0	-201 ± 7	24
	/L ₂ H	44.5 ± 3.9	-163 ± 12	43.1 ± 1.8	-197 ± 6	
	/L ₃ H	52.2 ± 3.4	-143 ± 11	47.6 ± 1.9	-184 ± 6	
[Pt(bpy)(H ₂ O) ₂]	/L ₁ H	15.3 ± 0.4	-204 ± 1	40.5 ± 0.7	-185 ± 2	This work
	/L ₂ H	22.2 ± 0.8	-185 ± 3	49.8 ± 1.2	-158 ± 4	
	/L ₃ H	26.5 ± 2.0	-173 ± 5	72.6 ± 4.9	-89 ± 15	

From the temperature dependence of the k_1 and k_2 values the activation parameters were calculated: $\Delta H_1^\ddagger = 15.3 \pm 0.4$ kJ mol⁻¹, $\Delta S_1^\ddagger = -204 \pm 1$ J K⁻¹ mol⁻¹ (for L₁H), $\Delta H_1^\ddagger = 22.2 \pm 0.8$ kJ mol⁻¹, $\Delta S_1^\ddagger = -185 \pm 3$ J K⁻¹ mol⁻¹ (for L₂H) and $\Delta H_1^\ddagger = 26.5 \pm 2.0$ kJ mol⁻¹, $\Delta S_1^\ddagger = -173 \pm 5$ J K⁻¹ mol⁻¹ (for L₃H) respectively. There occurs the formation of five member ring structure of the product by the coordination of two nitrogen atoms of LH with the Pt(II) center. One nitrogen atom first attacks one of the Pt(II) centre by the removal of one water molecule (k_1 path) and another nitrogen atom of the LH finishes the ring closing process (k_2 path) by the removal of second water molecule. Based on the above experimental findings, we propose the following reaction mechanism (Fig. 6).

Conclusions

From a comparison of the ligands used, it can be concluded that the variation in bulkiness and electronic effect of the entering vicinal-dioximes reflects their properties as nucleophiles and their reactivity follows the order: L₃H < L₂H < L₁H. The sensitivity of the reaction rate towards donor properties of the entering ligands are in the line with that expected for an associative mode of activation. Due to the highest steric effect, the reactivity of the ligand (L₃H) was lowest which reflects in the rate constant values. The reactivity of the complexes follow the below trend: [Pt(bpy)(H₂O)₂](ClO₄)₂ >> [Pt(en)(H₂O)₂](ClO₄)₂ > [Pt(pipen)(H₂O)₂](ClO₄)₂. The above order was already expected on the basis of the pK_a values (viz., the obvious influence of the diamine spectator ligands on the reactivity of the Pt(II) center). Addition of π -acceptors to the complex results in an increased reactivity of the

Pt(II) center. The reactions with the Pt(pipen) complex were expected to be slower than that of Pt(en), as the Pt(II) center in Pt(pipen) is less electrophilic due to the positive inductive effect (i.e., +I effect) of the piperidine ring compared to that of ethylenediamine. Where as in case of Pt(bpy), where two pyridine rings are adjacent to each other, the rates increase significantly. This can be attributed to the stronger trans-effect of π -acceptors such as pyridine rings compared to the weak trans-effect of amines of the type NH₂R. These findings are also reflected in the pK_a values of the coordinated water molecules, since they decrease with an increasing number of pyridine rings. So higher the electrophilicity of the metal center, smaller is the activation enthalpy because of stabilization of transition state and hence the above order of reactivity has been observed.

Supplementary Data

Supplementary data associated with this article are available in the electronic form at [http://www.niscair.res.in/jinfo/ijca/IJCA_56A_\(06\)_760-767_SupplData.pdf](http://www.niscair.res.in/jinfo/ijca/IJCA_56A_(06)_760-767_SupplData.pdf).

Acknowledgement

The authors are grateful to The Department of Chemistry, The University of Burdwan, Burdwan, West Bengal, India for extending all types of co-operation and providing infrastructural amenities during this work. Authors are also thankful to UGC, and DST, New Delhi, India for their support in developing infrastructural facilities.

References

- 1 Giaccone G, *Drugs*, 59 (2000) 9.
- 2 Perez R P, *Eur J Cancer*, 34 (1998) 1535.
- 3 Chu G, *J Biol Chem*, 269 (1994) 787.

- 4 Kelland L R, *Drugs*, 59 (2000).
- 5 Jakupec M A, Galanski M, Arion V B, Hartinger C G & Keppler B K, *Dalton Trans*, (2008) 183.
- 6 Jung Y & Lippard S J, *Chem Rev*, 107 (2007) 1387.
- 7 Jakupec M A, Galanski M & Keppler B K, *Rev Physiol Biochem Pharmacol*, 146 (2003) 1.
- 8 Galanski M, Jakupec M A & Keppler B K, *Curr Med Chem*, 12 (2005) 2075.
- 9 Lebwohl D & Canetta R, *Eur J Cancer*, 34 (1998) 1522.
- 10 Appleton T G, *Coord Chem Rev*, 166 (1997) 313.
- 11 Judson I & Kelland L R, *Drugs*, 59 (2000) 29.
- 12 Cvitkovic E, *Semin Oncol*, 25 (1998) 1.
- 13 Fuertes M A, Castilla J, Alonso C & Perez J M, *Curr Med Chem Anticancer Agents*, 2 (2002) 539.
- 14 Kirschenbaum L J, Panda R K, Borish E T & Mentasti E, *Inorg Chem*, 28 (1989) 3623.
- 15 Hughes M N, *The Inorganic Chemistry of Biological processes*, (Wiley, New York) 1981.
- 16 Ozcan E & Mirzaoglu R, *Synth React Inorg Met-Org Chem*, 18 (1988) 559.
- 17 Lance K A, Goldsby K A & Busch D H, *Inorg Chem*, 29 (1990) 4537.
- 18 Nandi D, Ray S, Laskar S & Ghosh A K, *J Indian Chem Soc*, 90 (2013) 913.
- 19 Arpalahti J & Lehtikoinen P, *Inorg Chim Acta*, 159 (1989) 115.
- 20 Behnke G T & Nakamoto K, *Inorg Chem*, 7 (1968) 330.
- 21 Sillen L G, Martell A E & Bjerrum J, *Stability Constants of Metal ion Complexes*, (The Chemical Society, London) 1964.
- 22 Irving H M & Rossotti H S, *J Chem Soc*, (1954) 2904.
- 23 Nandi D, Chottopadhyay A, Ray S, Acharjee A, Sarkar(Sain) R, Laskar S & Ghosh A K, *Monatsh Chem*, 147 (2016) 1015.
- 24 Nandi D, Ray S, Karmakar P, Chottopadhyay A, Dey A, Sarkar (Sain) R & Ghosh A K, *J Chem Sci*, 130 (2018) 124.